

Sommerfeld's Integrals and Hallén's Integral Equation in Data Analysis for Horizontal Dipole Antenna above Real Ground

Farid Monsefi¹, Milica Rančić^{1,2}, Sergei Silvestrov¹, and Slavoljub Aleksić²

- ¹ Division of Applied Mathematics, UKK, Mälardalen University, MDH Västerås, Sweden
(e-mail: farid.monsefi, milica.rancic, sergei.silvestrov@mdh.se)
- ² Dept. of Theoretical Electrical Engineering, ELFAK, University of Niš Niš, Serbia
(e-mail: slavoljub.aleksic@elfak.ni.ac.rs)

Abstract. High frequency (HF) analysis of the horizontal dipole antenna above real ground, which is employed in this paper, is based on the electric-field integral equation method and formulation of the Hallén's integral equation solved for the current using the point-matching method. The Sommerfeld's integrals, which express the influence of the real ground parameters, are solved approximately. Influence of different parameters of the geometry and ground on current distribution and input admittance is investigated. Furthermore, the method validation is done by comparison to the full-wave theory based exact model, and available measured data.

Keywords: Horizontal dipole antenna, Hallén's integral equation, Point-matching method, Polynomial current approximation, Real ground, Sommerfeld's integrals.

1 Introduction

Increase of the radiation power in different frequency bands during the last decades, has called for a study of harmful effects of the radio frequency energy on the living organisms and electronic equipment. An accurate determination of the near field strength in the vicinity of higher-power transmitting antennas is necessary for assessing any possible radiation hazards. In that sense, it is of great importance to account for the influence of the finite ground conductivity on the electromagnetic field structure in the surroundings of these emitters. The estimation of this influence has been intensively studied by Wait and Spies[1], Popović[2], Bannister[3], Popović and Djurdjević[4], Popović and Petrović[5], Rančić and Rančić[7], [8], Rančić and Aleksić[9], [11], Rančić[10], Arnautovski-Toseva *et al.*[12], [13], Nicol and Ridd[14], and a number of approaches has been applied in that sense, ranging from the exact full-wave based ones (Popović and Djurdjević[4], Arnautovski-Toseva *et al.*[12], [13]) to different forms of approximate, less time-consuming ones (Wait and Spies[1], Popović[2], Bannister[3], Popović and Petrović[5], Rančić and Rančić[7], [8], Rančić and Aleksić[9], [11], Rančić[10]). Although the approximate methods

introduce a certain level of calculation error, their simplicity is of interest in the electromagnetic compatibility (EMC) studies. For that reason, finding an approximate, but satisfyingly accurate method applicable to wide range of parameters is often a goal of researches done in this field.

In this paper, the authors perform analysis of a thin horizontal dipole antenna (HDA) above lossy half-space (LHS) of known electrical parameters. The approach is based on the electric-field integral equation method, and formulation of the Hallén's integral equation (HIE), Balanis[6]. This equation is then solved for the current, which is assumed in a polynomial form Popović[2], using the point-matching method (PMM) (Balanis[6]). This way obtained system of linear equations involves improper Sommerfeld's integrals, which express the influence of the real ground, and are here solved approximately using simple, so-called OIA and TIA, approximations (Rančić and Rančić[7], [8], Rančić and Aleksić[9], [11], Rančić[10]). Both types of approximations are in an exponential form, and therefore, are similar to those obtained applying the method of images. It should be kept in mind that the goal of this approach is to develop approximations that have a simple form, whose application yields satisfyingly accurate calculations of the Sommerfeld's type of integrals, and are widely applicable, i.e. their employment is not restricted by the values of electrical parameters of the ground, or the geometry, Rančić and Rančić[7], [8], Rančić and Aleksić[9], [11], Rančić[10].

Thorough analysis is performed in order to observe the influence of different parameters of the geometry, and the ground, on current distribution and the input impedance/admittance of the HDA. Furthermore, the verification of the method is done by comparison to the exact model based on the full-wave theory (Arnautovski-Toseva *et al.*[12], [13]), and experimental data from Nicol and Ridd[14]. Obtained results indicate a possibility of applying the described methodology to inverse problems involving evaluation of electrical parameters of the ground (or detection of ground type change) based on measured input antenna impedance/admittance.

2 Theory

Considered HDA is positioned in the air (conductivity $\sigma_0 = 0$, permittivity ϵ_0 , permeability μ_0) at height h above semi-conducting ground that can be considered a homogeneous and isotropic medium of known electrical parameters. Antenna conductors are of equal length $l_1 = l_2 = l$ and cross-section radius $a_1 = a_2 = a$ ($a \ll l$ and $a \ll \lambda_0$, λ_0 – wavelength in the air). The HDA is fed by an ideal voltage generator of voltage U and frequency f , and is oriented along the x -axis.

For such antenna structure, the Hertz's vector potential has two components, i.e. $\mathbf{\Pi}_{00} = \Pi_{x00} \hat{x} + \Pi_{zx00} \hat{z}$, which are described, at an the arbitrary field point $M_0(x, y, z)$, by the following expressions:

$$\Pi_{x00} = \frac{1}{4\pi\sigma_0} \int_{-l}^l I(x') [K_0(r_{1k}) + S_{00}^h(r_{2k})] dx', \quad (1)$$

$$\Pi_{zx00} = \frac{1}{4\pi\sigma_0} \frac{\partial}{\partial x} \int_{-l}^l I(x') \int_{\alpha=0}^{\infty} \left[-\underline{n}^{-2} \tilde{T}_{z10}(\alpha) + \tilde{T}_{\eta10}(\alpha) \right] \frac{\tilde{K}_{00}(\alpha, r_{2k})}{u_0} d\alpha dx'. \quad (2)$$

where $I(x')$ - current distribution (x' - axis assigned to the HDA); γ_i - propagation constant and σ_i - equivalent complex conductivity of the i -th medium ($i = 0$ for the air, and $i = 1$ for the lossy ground); $\underline{n} = \gamma_1/\gamma_0 = \sqrt{\epsilon_{r1}}$ - complex refractive index ($\gamma_0 = j\beta_0$ in the air); $\epsilon_{r1} \approx \epsilon_{r1} - j60\sigma_1\lambda_0$ - complex relative permittivity; α - continual variable over which the integration is done; $\tilde{K}_{00}(\alpha, r_{2k})$ - spectral form of the potential kernel, $K_0(r_{ik}) = e^{-\gamma_0 r_{ik}}/r_{ik}$ - standard potential kernel, $i = 1, 2$; $S_{00}^h(r_{2k})$ - a type of the Sommerfeld's integral; $\tilde{T}_{z10}(\alpha)$ and $\tilde{T}_{\eta10}(\alpha)$ - spectral transmission coefficients; $r_{1k} = \sqrt{\rho_k'^2 + (z-h)^2}$, $r_{2k} = \sqrt{\rho_k'^2 + (z+h)^2}$, $\rho_k' = (x-x'_k)^2 + (y-y'_k)^2$, $k = 1, 2$; $u_0 = \sqrt{\alpha^2 + \gamma_0^2}$, x'_k and y'_k - coordinates of the k -th current source element.

Boundary condition for the total tangential component of the electric field vector must be satisfied at any given point on the antenna surface, i.e.:

$$E_x + U\delta(x) = 0, \quad -l \leq x \leq l, \quad y = a, \quad z = h, \quad (3)$$

where E_x - x -component (tangential one) of the electric field vector \mathbf{E}

$$E_x = \mathbf{E}\hat{x} = \left[\text{graddiv } \mathbf{\Pi}_{00} - \gamma_0^2 \mathbf{\Pi}_{00} \right] \hat{x} = \frac{\partial^2 \Pi_{x00}}{\partial x^2} + \frac{\partial^2 \Pi_{zx00}}{\partial x \partial z} - \gamma_0^2 \Pi_{x00}. \quad (4)$$

The second term in (4) can be written in the following manner:

$$\frac{\partial^2 \Pi_{zx00}}{\partial x \partial z} = \frac{\partial^2 \Pi_{zx00}^*}{\partial x^2}, \quad (5)$$

where Π_{zx00}^* denotes the modified z -component of the Hertz's vector potential

$$\begin{aligned} \Pi_{zx00}^* &= \frac{-1}{4\pi\sigma_0} \int_{-l}^l I(x') \int_{\alpha=0}^{\infty} \left[-\underline{n}^{-2} \tilde{T}_{z10}(\alpha) + \tilde{T}_{\eta10}(\alpha) \right] \tilde{K}_{00}(\alpha, r_{2k}) d\alpha dx' = \\ &= \frac{-1}{4\pi\sigma_0} \int_{-l}^l I(x') \left[(1 - \underline{n}^{-2}) K_0(r_{2k}) - \underline{n}^{-2} S_{00}^v(r_{2k}) + S_{00}^h(r_{2k}) \right] dx \end{aligned} \quad (6)$$

where $S_{00}^v(r_{2k})$ - another type of the Sommerfeld's integral. Substituting (4) into (3) and adopting (5), the boundary condition (3) becomes:

$$\gamma_0^2 \Pi_{x00}^* - \frac{\partial^2 \Pi_{x00}^*}{\partial x^2} = \gamma_0^2 \Pi_{zx00}^* + U\delta(x), \quad -l \leq x \leq l, \quad y = a, \quad z = h, \quad (7)$$

where Π_{x00}^* denotes the *modified* x -component of the Hertz's vector potential

$$\begin{aligned} \Pi_{x00}^* &= \Pi_{x00} + \Pi_{zx00}^* = \\ &= \frac{1}{4\pi\sigma_0} \int_{-l}^l I(x') [K_0(r_{1k}) + (\underline{n}^{-2} - 1)K_0(r_{2k}) + \underline{n}^{-2}S_{00}^v(r_{2k})] dx'. \end{aligned} \quad (8)$$

Equation (7) presents the second order nonhomogeneous partial differential equation whose solution can be expressed as:

$$\begin{aligned} \Pi_{x00}^* &= C_1' \cos \beta_0 x + C_2' \sin \beta_0 x - \\ &- \frac{1}{\beta_0} \int_{s=0}^x [\gamma_0^2 \Pi_{zx00}^* + U\delta(x)] \Big|_{\substack{y=a \\ z=h}}^{x=s} \sin \beta_0(x-s) ds, \end{aligned} \quad (9)$$

i.e.

$$\begin{aligned} 4\pi\sigma_0\Pi_{x00}^* &= C_1 \cos \beta_0 x + C_2 \sin \beta_0 x + \\ &+ j\gamma_0 \int_{-l}^l I(x') \int_{s=0}^x \left[\begin{array}{c} (1-\underline{n}^{-2})K_0(r_{2k})- \\ -\underline{n}^{-2}S_{00}^v(r_{2k})+ \\ +S_{00}^h(r_{2k}) \end{array} \right] \Big|_{\substack{y=a \\ z=h}}^{x=s} \sin \beta_0(x-s) ds dx', \end{aligned} \quad (10)$$

where $C_1 = 4\pi\sigma_0 C_1'$, and $C_2 = 4\pi\sigma_0(C_2' - jU/\gamma_0)$ is a constant that will be obtained from the potential gap condition $\varphi_{00}(x=0^+) - \varphi_{00}(x=0^-) = U$ at feeding points. The electric scalar potential can be expressed as:

$$\varphi_{00} = -\text{div}\mathbf{\Pi}_{000} = -\frac{\partial\Pi_{x00}}{\partial x} - \frac{\partial\Pi_{zx00}}{\partial z} = -\frac{\partial\Pi_{x00}}{\partial x} - \frac{\partial\Pi_{zx00}^*}{\partial x} = -\frac{\partial\Pi_{x00}^*}{\partial x}, \quad (11)$$

and substituting (10) in (11) we get

$$\begin{aligned} \varphi_{00} &= -j30C_1 \sin \beta_0 x + \frac{U}{2} \cos \beta_0 x - \\ &- j30 \frac{\partial}{\partial x} \int_{-l}^l I(x') \int_{s=0}^x \left[\begin{array}{c} (1-\underline{n}^{-2})K_0(r_{2k})- \\ -\underline{n}^{-2}S_{00}^v(r_{2k})+ \\ +S_{00}^h(r_{2k}) \end{array} \right] \Big|_{\substack{y=a \\ z=h}}^{x=s} \sin \beta_0(x-s) ds dx'. \end{aligned} \quad (12)$$

Knowing (12), the potential gap condition yields $C_2 = -jU/60$. Finally (10) is:

$$\begin{aligned} 4\pi\sigma_0\Pi_{x00}^* &= C_1 \cos \beta_0 x - j\frac{U}{60} \sin \beta_0 x + \\ &+ j\gamma_0 \int_{-l}^l I(x') \int_{s=0}^x \left[\begin{array}{c} (1-\underline{n}^{-2})K_0(r_{2k})- \\ -\underline{n}^{-2}S_{00}^v(r_{2k})+ \\ +S_{00}^h(r_{2k}) \end{array} \right] \Big|_{\substack{y=a \\ z=h}}^{x=s} \sin \beta_0(x-s) ds dx'. \end{aligned} \quad (13)$$

Expression (13) presents the Hallén's integral equation (HIE) (Balanis[6]), having the current distribution $I(x')$ and the integration constant C_1 as unknowns. With a suitable function chosen to approximate the current distribution, HIE (13) is transformed to a system of linear equations applying the point-matching method at so-called matching points along the antenna.

It is of great importance to select an appropriate approximation for the current distribution since it will affect the calculation accuracy of both the near- and the far-field characteristics. There is a variety of proposed functions in the literature, but the polynomial current approximation proposed in Popović[2] was repeatedly proven as a very accurate one when analysing different wire antenna structures, Popović[2], Popović and Djurdjević[4], Popović and Petrović[5], Rančić and Rančić[7], [8], Rančić[10], Rančić and Aleksić[9], [11]. The form that will be used in this paper is as follows:

$$I(x') = \sum_{m=0}^M I_m \left(\frac{x'}{l} \right)^m, \quad (14)$$

where I_m , $m = 0, 1, 2, \dots, M$, present unknown complex current coefficients. Adopting (14), HIE (13) becomes:

$$\sum_{m=0}^M I_m \int_{-l}^l \left(\frac{x'}{l} \right)^m \left[\begin{array}{c} K_0(r_{1k}) + (\underline{n}^{-2} - 1)K_0(r_{2k}) + \underline{n}^{-2}S_{00}^v(r_{2k}) - \\ \left[\begin{array}{c} (1 - \underline{n}^{-2})K_0(r_{2k}) - \\ -\underline{n}^{-2}S_{00}^v(r_{2k}) + \\ + S_{00}^h(r_{2k}) \end{array} \right]_{\substack{x=s \\ y=a \\ z=h}} \end{array} \right] \sin \beta_0(x-s) ds \Big] dx' - \\ -C_1 \cos \beta_0 x = -j \frac{U}{60} \sin \beta_0 x. \quad (15)$$

Unknown complex current coefficients I_m , $m = 0, 1, 2, \dots, M$, are determined from the system of linear equations obtained matching (15) at points:

$$x_i = \frac{i}{M}l, \quad i = 0, 1, 2, \dots, M. \quad (16)$$

This way, system of $(M + 1)$ linear equations is formed, lacking one additional equation to account for the unknown integration constant C_1 . This remaining linear equation is obtained applying the condition for the current at the conductor's end. Standardly, the vanishing of the current is assumed at the end of antenna arm (Popović[2], Popović and Djurdjević[4], Popović and Petrović[5], Rančić and Rančić[7], [8], Rančić and Aleksić[9], [11], Rančić[10]), which corresponds to $I(-l) = I(l) = 0$, i.e. based on (14) to

$$\sum_{m=0}^M I_m = 0. \quad (17)$$

(Note: A more realistic condition for the current at the conductor's ending, derived satisfying the continuity equation at the end of an antenna arm, can also be used.)

This way, the system of equations needed for computing the current distribution of the observed antenna is formed. Based on that, for the given generator voltage U , the input admittance is determined from $Y_{in} = I_0/U$, where $I_0 = I_m|_{m=0}$.

Remaining problem are two Sommerfeld's integrals appearing in (15) expressed by

$$S_{00}^v(r_{2k}) = \int_{\alpha=0}^{\infty} \tilde{R}_{z10} \tilde{K}_{00}(\alpha, r_{2k}) d\alpha, \quad (18)$$

$$S_{00}^h(r_{2k}) = \int_{\alpha=0}^{\infty} \tilde{R}_{\eta10} \tilde{K}_{00}(\alpha, r_{2k}) d\alpha, \quad (19)$$

where the first terms in both integrands represent spectral reflection coefficients (SRCs):

$$\tilde{R}_{z10}(\alpha) = \frac{\underline{n}^2 u_0 - u_1}{\underline{n}^2 u_0 + u_1}, \quad u_i = \sqrt{\alpha^2 + \underline{\gamma}_i^2}, \quad i = 0, 1, \quad (20)$$

$$\tilde{R}_{\eta10}(\alpha) = \frac{u_0 - u_1}{u_0 + u_1}, \quad u_i = \sqrt{\alpha^2 + \underline{\gamma}_i^2}, \quad i = 0, 1. \quad (21)$$

In order to solve the type of Sommerfeld's integral given by (18) the methodology proposed in Rančić and Rančić[7] will be applied. Let us assume the SRC (20) in a so-called - TIA (*two-image approximation*) form:

$$\tilde{R}_{z10}(u_0) \cong B_v + A_{1v} e^{-(u_0 - \underline{\gamma}_0) \underline{d}_v}, \quad (22)$$

where B_v , A_{1v} and \underline{d}_v are unknown complex constants. When (22) is substituted into (18), the following general TIA approximation is obtained:

$$S_{00}^v(r_{2k}) \cong B_v K_0(r_{2k}) + A_v K_0(r_{2kv}), \quad (23)$$

where $r_{2kv} = \sqrt{\rho_k^2 + (z + h + \underline{d}_v)^2}$, presents the distance between the second image and the observation point M_0 , and $A_v = A_{1v} \exp(\underline{\gamma}_0 \underline{d}_v)$. Now, matching expressions (20) and (22) at $u_0 \rightarrow \infty$ and $u_0 = \underline{\gamma}_0$, and the first derivative of the same expressions at $u_0 = \underline{\gamma}_0$, the following values for the unknown complex constants in (22) are obtained:

$$B_v = R_\infty, \quad A_{1v} = R_0 - R_\infty, \quad \underline{d}_v = (1 + \underline{n}^{-2}) / \underline{\gamma}_0, \quad (24)$$

where: $R_\infty = \tilde{R}_{z10}(u_0 \rightarrow \infty) = (\underline{n}^2 - 1) / (\underline{n}^2 + 1)$ and $R_0 = (\underline{n} - 1) / (\underline{n} + 1)$.

Substituting (24) into (23), the following TIA form of (18) is obtained:

$$S_{00}^v(r_{2k}) \cong R_\infty K_0(r_{2k}) + (R_0 - R_\infty) e^{\underline{\gamma}_0 \underline{d}_v} K_0(r_{2kv}). \quad (25)$$

Similarly, we can assume (21) in the following form (Rančić and Rančić[8], Rančić and Aleksić[9], [11], Rančić[10]):

$$\tilde{R}_{\eta10}(u_0) \cong B_h + A_{1h} e^{-(u_0 - \underline{\gamma}_0) \underline{d}_h}, \quad (26)$$

where B_h , A_{1h} and \underline{d}_h - unknown complex constants. Substituting (26) into (19), the following general approximation is obtained:

$$S_{00}^h(r_{2k}) \cong B_h K_0(r_{2k}) + A_h K_0(r_{2kh}), \quad (27)$$

where $A_h = A_{1h} \exp(\gamma_0 d_h)$, and $r_{2kh} = \sqrt{\rho_k^2 + (z + h + d_h)^2}$.

After matching (21) and (26) at points $u_0 \rightarrow \infty$ and $u_0 = \gamma_0$, and their first derivatives at $u_0 = \gamma_0$, we get values $B_h = 0$, $A_{1h} = -R_0$, and $\underline{d}_h = 2/(\gamma_0 n)$, i.e. (27) gets the OIA (*one-image approximation*) form, Rančić and Aleksić[9], [11], Rančić[10]:

$$S_{00}^h(r_{2k}) \cong -R_0 e^{\gamma_0 d_h} K_0(r_{2kh}). \quad (28)$$

3 Numerical results

Described numerical procedure is applied to near-field analysis of the symmetrical HDA fed by an ideal voltage generator of voltage U .

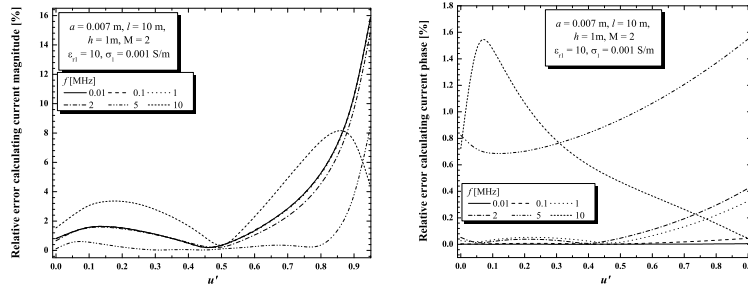


Fig. 1. Relative error of the current magnitude (left) and phase (right) along the HDA arm.

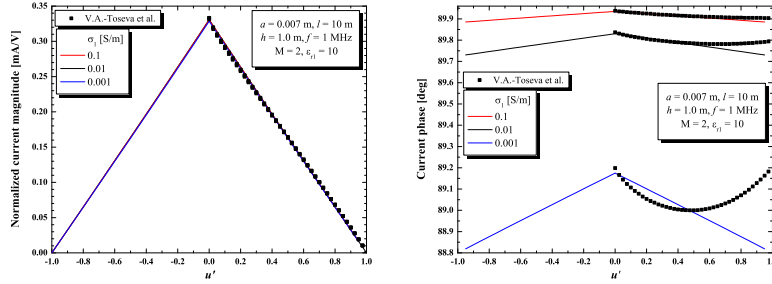


Fig. 2. Current magnitude (left) and phase (right) along the HDA for different ground conductivities.

Firstly, results of the relative error of current distribution calculation are given in Figure 1. The conductor is $2l = 20$ m long with the cross-section

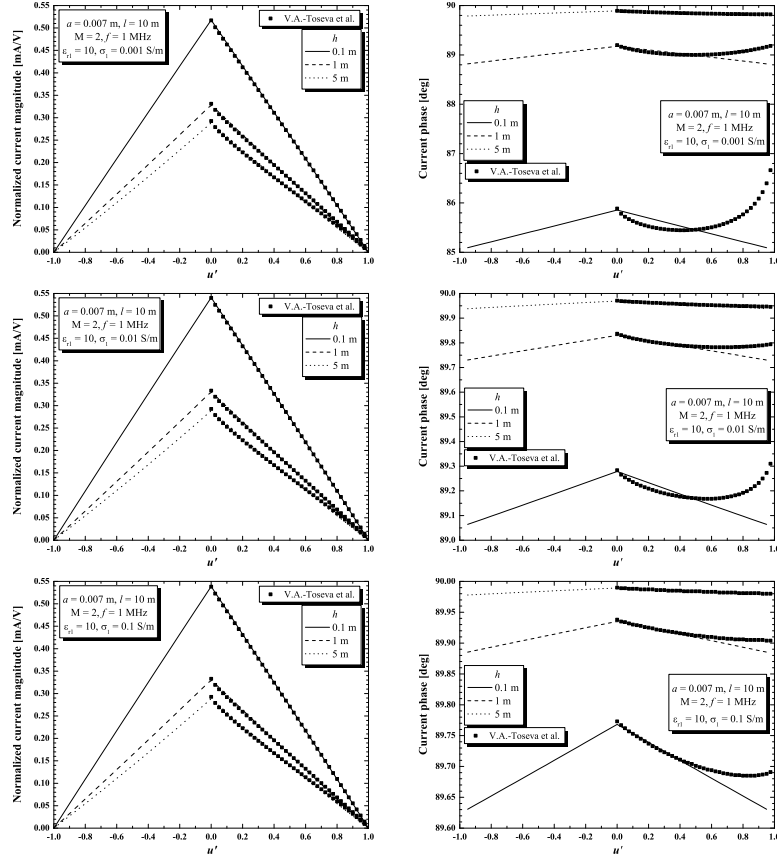


Fig. 3. Current magnitude (left) and phase (right) along the HDA above LHS at different heights.

radius of $a = 0.007$ m, and it is placed at $h = 1.0$ m above lossy ground with electrical permittivity $\epsilon_{r1} = 10$. In this case, the variable parameter is the frequency that takes values from a wide range (10 kHz to 10 MHz). The relative error is shown separately for the current magnitude and phase along the HDA arm for the case of the specific conductivity of $\sigma_1 = 0.001$ S/m. As a reference set of data, those from Arnautovski-Toseva *et al.*[12], [13] are taken.

Current distribution's magnitude and phase at 1 MHz, can be observed from Figure 2. The HDA has the same dimensions as previously, and it is placed at $h = 1.0$ m above lossy ground with electrical permittivity $\epsilon_{r1} = 10$. The value of the specific conductivity has been taken as a parameter: $\sigma_1 = 0.001, 0.01, 0.1$ S/m. Comparison has been done with the results from Arnautovski-Toseva *et al.*[12], [13].

Further, the influence of the conductor's position on the current distribution has been analysed. The results are graphically illustrated in Figure 3 together with the ones from Arnautovski-Toseva *et al.*[12], [13]. Three cases were observed that correspond to heights $h = 0.1, 1.0, 5.0$ m. The current has been calculated at frequency of 1 MHz, and analysis has been done for the following values of the specific ground conductivity: $\sigma_1 = 0.001, 0.01, 0.1$ S/m. HDA dimensions are the same as previously.

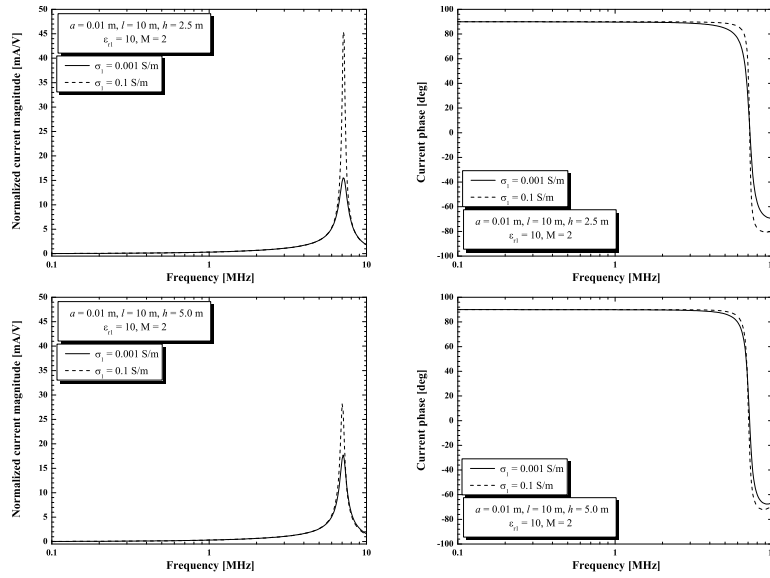


Fig. 4. HDA current magnitude (left) and phase (right) at point A for different ground conductivities.

Next example explores the dependence of the current (its magnitude and phase) on different ground conductivities calculated at the feeding point A ($l = 0$ m), which can be observed from Figure 4. Two cases are considered: solid line represents the value of $\sigma_1 = 0.001$ S/m, and the dashed one corresponds to $\sigma_1 = 0.1$ S/m. The first row of Figure 4 corresponds to HDA height of $h = 2.5$ m, and the second one to $h = 5.0$ m. The same influence for height $h = 0.5$ m is given in Rančić and Aleksić[11].

Similarly, the dependence of the current (its magnitude and phase) at specific points along the HDA arm in the frequency range from 10 kHz to 10 MHz, is presented in Figure 5. The antenna is $2l = 20$ m long with a cross-section radius of $a = 0.01$ m, and considered heights are: $h = 0.5, 2.5, 5.0$ m. Electrical parameters' values of the ground are: electrical permittivity $\epsilon_{r,1} = 10$, and specific conductivity $\sigma_1 = 0.1$ S/m. Current is calculated at points:

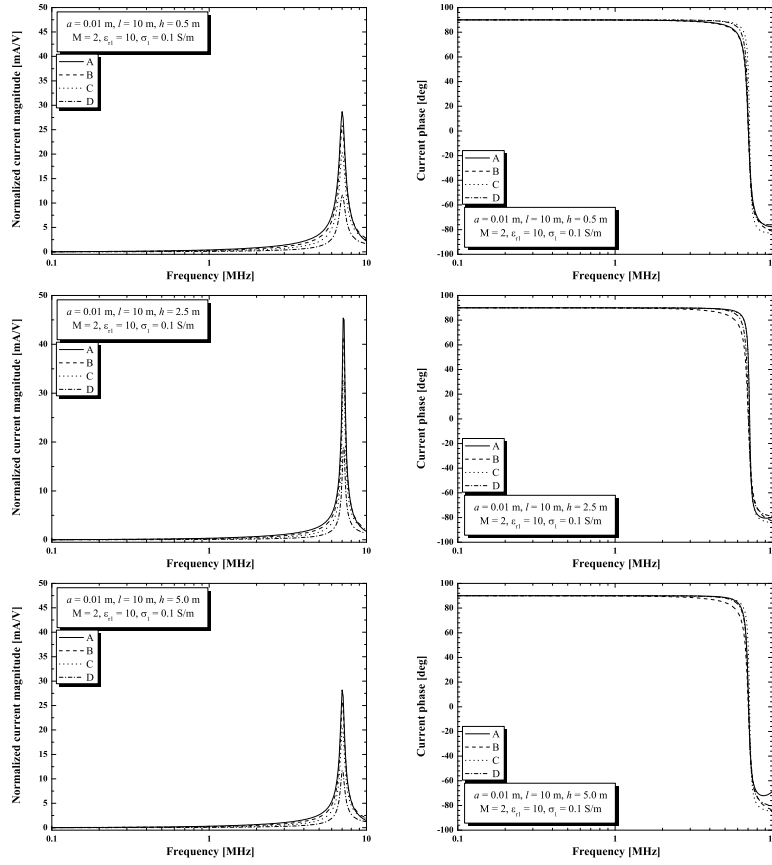


Fig. 5. HDA current magnitude (left) and phase (right) at different points along the antenna.

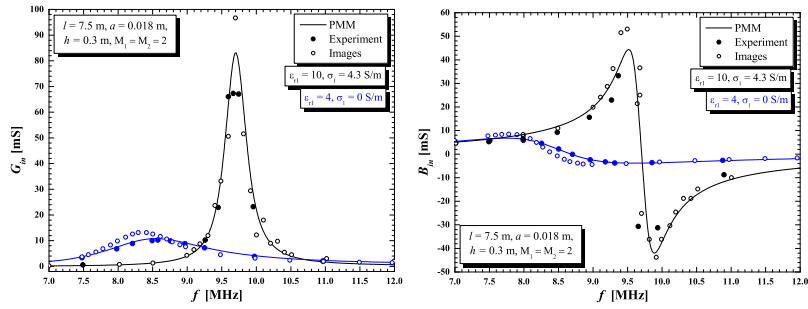


Fig. 6. HDA input conductance (left) and susceptance (right) versus frequency.

A($l = 0$ m), B($l = 2.5$ m), C($l = 5.0$ m), and D($l = 7.5$ m). This example for $\sigma_1 = 0.001$ S/m and $h = 0.5$ m is given in Rančić and Aleksić[11].

Finally, Figure 6 shows comparison between theoretical calculations performed using the methodology described in this paper, and the results of the admittance measurements for the frequency range of 7 – 12 MHz (Nicol and Ridd[14]). Observed HDA is 15 m long suspended at height of 0.3 m above the LHS. Two boundary cases of the ground are observed: a perfect dielectric (blue data), and a highly conducting plane (black data). Corresponding results obtained by the method of images are also shown (open circles). It can be observed that the better accordance is achieved using the method described here, which was expected since the observed antenna is very close to the ground (for the frequency of 10 MHz, height of 0.3 m corresponds to $0.01\lambda_0$), and the accuracy of the method of images decreases when the antenna is at height less than $h/\lambda_0 = 0.025$ (Popović and Petrović[5]).

4 Conclusions

Approximate method for the analysis of horizontal dipole antenna has been applied in this paper for the purpose of the current distribution and input admittance evaluation for the HDA positioned in the air at arbitrary height above LHS, which is considered a homogenous medium. The aim of the paper was to validate the applied method for the cases of interest in the EMC studies.

The analysis has been performed in a wide frequency range, and for different positions of the antenna, as well as for various values of the LHS's conductivity. It has been proven, based on the comparison with the exact model from Arnautovski-Toseva *et al.*[12], [13], that the methodology used here yields very accurate results in the observed parameters' ranges. This indicates a possibility of applying this method for analysis of different wire structures in the air above LHS, and more importantly, very close to the ground where the finite conductivity's influence is the greatest.

5 Acknowledgement

This work is partly supported by the RALF3 project funded by the Swedish Foundation for Strategic Research (SSF), and the EUROWEB Project funded by the Erasmus Mundus Action II programme of the European Commission.

The second author would like to thank members of the Division of Applied Mathematics at the MDH University, Sweden for inspiring and fruitful collaboration.

References

1. Wait, J. R. and Spies, K. P., "On the Image Representation of the Quasi-Static Fields of a Line Current Source above the Ground", *Can. J. Phys.* 47, 2731–2733 (1969).
2. Popović, B. D., "Polynomial Approximation of Current along thin Symmetrical Cylindrical Dipoles", *Proc. Inst. Elec. Eng.* 117, 5, 873–878 (1970).
3. Bannister, P. R., "Extension of Quasi-Static Range of Finitely Conducting Earth Image Theory Technique to other Ranges", *IEEE Trans. on AP* 26, 3, 507-508 (1978).
4. Popović, B. D. and Djurdjević, D. Ž., "Entire-Domain Analysis of Thin-Wire Antennas near or in Lossy Ground", *IEE Proc., Microw. Antennas Propag.* 142, 213-219 (1995).
5. Popović, B. D. and Petrović, V. V., "Horizontal Wire Antenna above Lossy Half-Space: Simple Accurate Image Solution", *International journal of numerical modelling: Electronic networks, devices and fields* 9, 194-199 (1996).
6. Balanis, C. A., *Antenna Theory: Analysis and Design, Chapter 8*, 3rd Edition: J. Wiley Sons, Inc., Hoboken, New Jersey (2005).
7. Rančić, M. P. and Rančić, P. D., "Vertical Dipole Antenna above a Lossy Half-Space: Efficient and Accurate Two-Image Approximation for the Sommerfeld's Integral", in Proc. of *EuCAP 2006* Nice, France, paper No121 (2006).
8. Rančić, M. and Rančić, P., "Horizontal Linear Antennas above a Lossy Half-Space: A New Model for the Sommerfeld's Integral Kernel", *Int. J. El. Commun. AEU* 65, 879-887 (2011).
9. Rančić, M. and Aleksić, S., "Horizontal Dipole Antenna very Close to Lossy Half-Space Surface", *Electrical Review* 7b, 82-85 (2012).
10. Rančić, M., *Analysis of Wire Antenna Structures in the Presence of Semi-Conducting Ground*, Ph.D dissertation, Faculty of electronic engineering, University of Niš, Niš, Serbia (2012).
11. Rančić, M. and Aleksić, S., "Analysis of Wire Antenna Structures above Lossy Homogeneous Soil", in Proc. of *21st Telecommunications Forum (TELFOR)* Belgrade, Serbia, 640-647 (2013).
12. Arnautovski-Toseva, V., Khamlichi Drissi, K. El, and Kerroum, K., "Comparison of Approximate Models of Horizontal Wire Conductor above Homogeneous Ground", in Proc. of *EuCAP 2012* Prague, Czech Republic, 678-682 (2012).
13. Arnautovski-Toseva, V., Khamlichi Drissi, K. El, Kerroum, K., Grceva, S. and Grcev, L., "Comparison of Image and Transmission Line Models of Energized Horizontal Wire above Two-Layer Soil", *Automatika* 53, 38-48 (2012).
14. Nicol, J.L. and Ridd, P.V., "Antenna Input Impedance: Experimental Confirmation and Geological Application", *Can. J. Phys.* 66, 818-823 (1988).